

---

# IMPLEMENTATION STUDY OF COST-EFFECTIVE VERIFICATION FOR PIETRZAK'S VERIFIABLE DELAY FUNCTION IN ETHEREUM SMART CONTRACTS

---

A PREPRINT

**Suhyeon Lee** <sup>§</sup>  
Tokamak Network  
suhyeon@tokamak.network

**Euisin Gee** <sup>§</sup>  
School of Cybersecurity  
Korea University  
usgee@korea.ac.kr  
Onther  
justin.g@onther.io

**Junghee Lee**  
School of Cybersecurity  
Korea University  
j\_lee@korea.ac.kr

May 13, 2024

## ABSTRACT

Verifiable Delay Function (VDF) is a cryptographic concept that ensures a minimum delay before output through sequential processing, which is resistant to parallel computing. Among the two well-known VDF protocols, Wesolowski and Pietrzak VDF, we focus on the Pietrzak VDF due to its computational efficiency and suitability for blockchain environments. Pietrzak's approach uses a recursive proof verification with the halving protocol, offering a practical alternative despite the longer proof length than Wesolowski's approach. Given the scarcity of research on practical VDF verification implementation, especially within smart contracts, this paper aims to implement cost-effective verification for the Pietrzak VDF in an Ethereum-based environment without compromising the VDF verification's integrity and reliability. Firstly, we propose generalized proof generation and verification algorithms for potential efficiency improvement. Secondly, we categorize and measure the gas cost of each part in a transaction for VDF verification. Thirdly, based on the analysis, we theoretically predict the optimized proof construction. Finally, we demonstrate the theoretical prediction matches the implementation results. Furthermore, our research shows that the proof length of the Pietrzak VDF is generated under 8 KB with the security level of 2048 bits, much smaller than the previous expectation. This implies that the Pietrzak VDF can be practically used for cryptographic applications on blockchains.

**Keywords** Ethereum · blockchain security · cryptographic protocol · decentralized application · gas optimization · verifiable delay function

## 1 Introduction

In blockchain technology, one critical element is the generation and use of cryptographically secure random numbers. These secure random numbers play a pivotal role in various applications of blockchain; for example, in consensus, random numbers can ensure fair selections of sequencers and block proposers based on a probabilistic process. Random numbers are essential for ensuring anonymity and serve as the basis for cryptographic techniques. Despite the significance of secure random numbers, incorporating them into smart contracts results in challenges. Due to the lack of random number methods in the smart contract interface, individuals previously used to apply future block data (i.e. the blockhash of a future block) as an ad-hoc random number. It can be manipulated by a block generator. Hence, leveraging ad-hoc random numbers is not a suitable approach for the present situation.

---

<sup>§</sup>These authors contributed equally to this work.

We express our special thanks to Prof. Seungjoo Kim at Korea University for his invaluable advice on cryptographic algorithms.

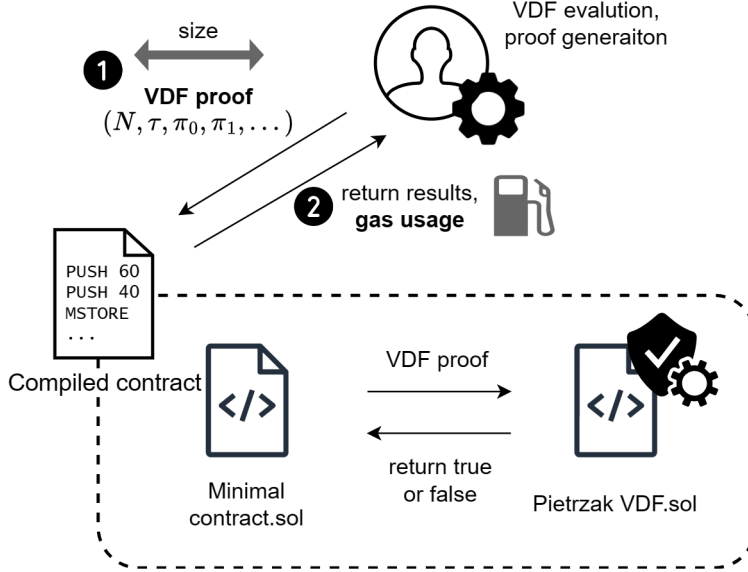


Figure 1: In our model, a user sends a VDF proof after the Pietrzak VDF evaluation. The primary issue is the significant gas usage for the VDF verification. The secondary issue is the length of the VDF proof as the Pietrzak VDF’s length increases as the time delay increases.

In this context, two notable techniques have emerged: Verifiable Random Functions (VRFs) and Verifiable Delay Functions (VDFs). VRFs are cryptographic primitives that produce a random number along with proof of its correctness, allowing anyone to verify the number’s authenticity without compromising its unpredictability. Several commercial random number generating services using VRF, such as Chainlink VRF, are already available. As part of their operation, a node acting as an oracle transmits a randomly generated number from off-chain nodes to a blockchain.

On the other hand, VDFs are designed to produce a unique output that requires a predetermined amount of time to compute, but whose result can be efficiently verified by others. Therefore, VDFs do not directly generate a random number. Rather, VDFs support random number generation of the commit-reveal scheme by utilizing their time-lock property. The most critical weakness of the commit-reveal scheme is that all the participants must reveal to generate a secure random number. VDFs’ time-lock property ensures that the random outcome cannot be predicted or accelerated by computational power in case of any absence. It makes VDFs practical for applications that benefit from a guaranteed delay in randomness generation. Considering financial penalties do not perfectly guarantee the generation of random numbers, the commit-reveal scheme can enhance security with VDFs as a commit-reveal-recover scheme.

Pivotal advancements in VDFs have been made through the research of Pietrzak [1] and Wesolowski [2], who each proposed practical implementations of VDFs. Despite these theoretical developments, there remains a notable gap in research regarding the application of VDFs within blockchain environments. The challenge lies not only in the theoretical construction of VDFs, but also in adapting these constructions to the resource usage context of blockchain systems. For example, the Pietrzak VDF uses the halving protocol that makes the length of proof proportional to the delay time. It makes utilizing the Pietrzak VDF considered unrealistic in blockchain [3]. The Wesolowski VDF needs a hash-to-prime oracle that is not supported in most blockchains.

When implementing VDFs, the process can broadly be divided into three parts: evaluation, proof generation, and verification. In the context of blockchain, the verification component must be implemented on-chain. This segmentation is due to our belief that in typical blockchain applications, both evaluation and proof generation processes are performed off-chain, mainly due to their computational intensity and the associated costs when executed on a blockchain network.

Our goal has been to efficiently implement VDF verification within smart contracts as Figure 1’s illustration. Specifically, we have targeted the Pietrzak VDF model. There are two reasons: Firstly, the Wesolowski VDF requires a hash-to-prime function that is challenging to implement on smart contracts. Secondly, we conjectured that optimization can mitigate the long-proof length issue partially. Based on this algorithm choice, consequently, this research demonstrated that the Pietrzak VDF verification can be utilized in the EVM-compatible smart contract environment through various cost-saving analysis and experiments.

The contributions of this paper are as follows:

- To the best of our knowledge, this research presents the first academic study of Pietrzak VDF implementation on smart contracts.
- We proposed generalized algorithms for proof generation and verification of the Pietrzak VDF for potential efficiency enhancement.
- Through theoretical analysis, we demonstrated the existence of a unique parameter that reduces the proof length. Additionally, the actual implementation results were consistent with our theoretical expectations.
- Contrary to previous studies' expectations, we demonstrated that the Pietrzak VDF could be utilized in the Ethereum environment with under 10 KB calldata size.

The rest of the paper is organized as follows: Section 2 introduces related studies about VDFs and their implementation. Section 3 describes the proposed target algorithms and our implementation environment. Section 4 illustrates the data structures of proofs and analyzes gas costs for the data and its dispatching cost. Section 5 studies arithmetic operations in the verification process and their gas costs. In Section 6, based on the previous sections' outcomes, we present theoretical analysis and the cost-effective implementation. Section 7 discusses this research's contributions, limitations, and future directions. Finally, Section 8 concludes the paper.

## 2 Background

This section introduces VDFs, cryptographic algorithms crucial for blockchain applications and secure timestamping. It also reviews related works that inform the VDF implementations discussed in this paper.

### 2.1 Verifiable Delay Functions

VDFs are cryptographic protocols crafted to ensure that their execution takes a predefined minimum amount of time, regardless of the computational power applied. Here we introduce the core mechanisms that define VDFs and the core properties that VDFs get from the elements.

#### 2.1.1 Definition and Fundamental Properties

A VDF consists of three key algorithms that facilitate one round: setup, evaluation, and verification.

- **Setup** ( $\text{Setup}(1^\lambda) \rightarrow (\mathbb{G}, T)$ ): Initializes the VDF with public parameters. Here,  $1^\lambda$  represents the security parameter indicating the required security level,  $\mathbb{G}$  is a cryptographic group used in computations, and  $T$  is the time delay parameter that sets the duration of the computation.
- **Evaluation** ( $\text{Evaluate}(\mathbb{G}, T, X) \rightarrow (Y, \pi)$ ): For a given input  $X$ , the VDF computes an output  $Y$  over time  $T$ , which is deliberately designed to be sequential, preventing acceleration through parallel processing. The output includes a proof  $\pi$  that validates the computation.
- **Verification** ( $\text{Verify}(\mathbb{G}, T, X, Y, \pi) \rightarrow \{\text{true}, \text{false}\}$ ): Enables any observer to quickly and efficiently verify the correctness of the output  $Y$  and its proof  $\pi$  without undergoing the time-intensive computation themselves. A return of **true** confirms the validity of the output, while **false** indicates an error.

From the above algorithms, VDFs must get the three primary attributes [4]:

- **Sequentiality in evaluation:** The computation must take a fixed minimum time, irrespective of the available computational resources.
- **Efficiency in verification:** Although the computation itself is intentionally delayed, the verification process is designed to be quick and require minimal resources.
- **Uniqueness in output:** Each input to a VDF yields a unique, unpredictable output, ensuring reliability and consistency in applications.

### 2.2 Feasibility of Applying VDFs to Smart Contracts

In both Wesolowski [2] and Pietrzak [1], the prover claims  $y = x^{2^T} \bmod N$  where  $N$  is a RSA modulus, but the way to verify it is different. In Wesolowski, the verifier gives the prover a random and large prime challenge value  $c$ , and the prover gives the verifier a proof  $\pi$  which is  $x^{2^T/c}$ . Here, the prover does not compute  $\pi$  anew but rather responds by taking the intermediate value of the process of computing  $y = x^{2^T} \bmod N$  from memory. The verifier then checks

if  $\pi \in \mathbb{Z}_N^*$  and accepts if  $y = \pi^c x^{2^T \bmod c}$ . To make this scheme non-interactive in a blockchain environment, the Fiat-Shamir heuristic is utilized: the prover computes  $c$  directly as  $\text{hash-to-prime}(x, y)$  and passes it along with  $\pi$  to the verifier in the first message. To ensure the difficulty in creating a verifiable proof, it is computationally assumed that calculating  $z^c = y \bmod N$  is challenging for any  $z \neq 1$ . Although this operation is time-independent with respect to  $T$ , it requires considerable resources and presents significant implementation challenges. These include incorporating an on-chain hash-to-prime function capable of handling relatively large data sizes, such as 2048 bits.

On the other hand, Pietrzak VDF does not require techniques like hash-to-prime and makes no computational assumptions. In the Pietrzak protocol, proof generation and verification are halving protocol that involves a loop  $\log(T)$  times, dividing  $T$  by 2 until  $T$  becomes 1. During each iteration of the loop in a proof generation, the prover computes  $v_i = x^{2^{T/2}}$ . The Fiat-Shamir heuristic is used to compute  $r = \text{Hash}(x_i, y_i, v_i)$  to make it non-interactive in a blockchain environment. And the prover and verifier calculate  $(x_{i+1}, y_{i+1}) \leftarrow (x_i^r v_i, v_i^r y_i)$  that satisfies  $y_{x+i} = x_{i+1}^{2^{T/2}}$ . Thus, a proof  $\pi = \{v_i\}_{i \in [1, \log_2 T]}$  of  $\log_2 T$  length is produced. When each element of the proof is over 2048 bits, it is expected to be impractical for use in a blockchain due to the large size [3].

### 2.3 Related Works

In this subsection, we review the critical advancements in VDFs, from their theoretical foundations to practical implementations related to this study.

**Theoretical research on VDFs.** The concept of VDFs has garnered significant attention for its potential to enable new applications in cryptography and blockchain technology. The foundational work by Rivest, Shamir, and Wagner on "Time-Lock Puzzles and Timed-Release Crypto" [5] laid the groundwork for the development of protocols that secure data until a certain amount of time has passed. This seminal paper introduced the concept of time-lock puzzles, a precursor to VDFs, demonstrating how cryptographic operations could be used to create a delay mechanism that is practically infeasible to bypass without solving the puzzle.

Building upon these principles, Pietrzak [1] and Wesolowski [2] independently proposed two distinct approaches to VDFs, each with unique advantages in terms of efficiency and security. Pietrzak's method focuses on using iterated sequential squaring in a group of unknown order, providing a balance between computation time and verification efficiency. Wesolowski's approach, on the other hand, introduces an elegant solution that reduces the verification complexity, making it more practical for applications that require fast and efficient verification processes.

Further advancing the field, Dan Boneh et al. [6] have conducted extensive research on optimizing VDFs, addressing critical aspects such as the construction of more efficient protocols and the reduction of computational requirements for both generation and verification phases. Their work not only highlights the theoretical advancements in VDF technology but also emphasizes the practical implications for secure, decentralized systems.

**Implementation of VDFs.** The practical realization of VDFs has become an area of intense research and development, seeking to bridge the gap between theoretical robustness and real-world applicability. A significant contribution to this endeavor is the study by Attias et al. [3], which provides a comprehensive implementation analysis of two leading VDFs, Pietrzak and Wesolowski. Their work meticulously evaluates the performance of VDFs' evaluation, proof generation, and verification. Their work provided us with insight into the research and optimization techniques for VDFs. However, they expected the Pietrzak VDF would not be viable for blockchains. This is contrary to our results that presented the feasibility of the Pietrzak VDF on Ethereum smart contracts.

Choi et al. [7] proposed three practical commit-reveal-recover techniques. Their protocols are crucial for establishing the commit-reveal-recover scheme, which mostly existed at the conceptual level. They incorporated the Wesolowski VDF into Ethereum smart contracts for the purpose of demonstration. Our research covers VDF verification, which corresponds to the Proof-of-Exponentiation (PoE) stated in their work. Their PoE gas usage is approximately 2.3 million, which is comparable to the gas consumption of our work with the time delay variable of  $2^{22}$ . Due to the Wesolowski VDF not having increased calculation requirements with greater time delays, our approach becomes less efficient when the time delay variable exceeds  $2^{23}$ . Nevertheless, the Wesolowski VDF encounters an issue when it comes to fully implementing the hash-to-prime function as previously indicated.

## 3 Implementation Target and Environment

In this section, we provide the target algorithm and environment. Firstly, we define the Pietrzak VDF algorithms we aim to implement in this research. Secondly, we describe the experiment environment in the following sections.

### 3.1 Pietrzak VDF Algorithms

Our research has a model with a smart contract that supports a function that performs Pietrzak VDF verification. Referring to the Pietrzak's original paper [1], we define the evaluation as described in Algorithm 1 and the halving protocol for proof generation in Algorithm 2.

#### 3.1.1 VDF Evaluation

$$y \equiv x^{2^T} \equiv x^{2^{2^T}} \pmod{N} \quad (1)$$

The VDF evaluation process as defined in Algorithm 1 is pivotal in generating a VDF output from given inputs. It basically computes Equation 1. The algorithm takes an initial value  $x$ , a time parameter  $T$  (also notated as  $2^T$ ), and a modulus  $N$  to produce the output  $y$ .  $N$  that is a  $\lambda$ -bit number is produced by an RSA setup ( $N = p \cdot q$  where  $p, q$  are two big prime numbers). The process involves exponentiating  $x$  to  $2^T \pmod{N}$  to ensure the difficulty and time consumption of the evaluation are as intended. This evaluation serves as the foundation for verifying that the output can only be computed with a predefined amount of real-time computational work, which is crucial in applications requiring guarantees against parallelization.

---

#### Algorithm 1 Evaluation of the Pietrzak VDF

---

```

1: input:  $x, T, N$ 
2: output:  $y$ 
3:  $y \leftarrow x$ 
4: for  $k \leftarrow 1$  to  $T$  do
5:    $y \leftarrow y^2 \pmod{N}$ 
6: end for
7: return  $y$ 

```

---

#### 3.1.2 Halving Protocol

The halving protocol detailed in Algorithm 2 optimizes the proof generation process for VDFs by reducing the verification time incrementally. At each step, the protocol halves the time parameter  $T$ , recalculates intermediate values  $x_i$  and  $y_i$ , and updates these values based on a cryptographic hash function to ensure integrity. As we implement it on Ethereum, we use Keccak256 as the cryptographic hash function. This iterative reduction continues until the desired granularity is reached, ensuring that the verifier's workload is minimized while maintaining cryptographic security.

---

#### Algorithm 2 Halving Protocol of the Pietrzak VDF

---

```

1: input:  $N, x_i, T, y_i$ 
2: output:  $N, x_{i+1}, T/2^i, y_{i+1}, \mu_{i+1}$ 
3:  $\mu_i \leftarrow x_i^{2^{T/2^i}}$ 
4:  $r_i \leftarrow \text{Hash}(x_i + y_i + v_i)$ 
5:  $x_{i+1} \leftarrow x_i^{r_i} \cdot v_i \pmod{N}$ 
6: if  $T/2^{i-1}$  is odd then
7:    $y_i \leftarrow y_i^2 \pmod{N}$ 
8: end if
9:  $y_{i+1} \leftarrow v_i^{r_i} \cdot y_i \pmod{N}$ 
10: return  $N, x_{i+1}, T/2^i, y_{i+1}, \mu_{i+1}$ 

```

---

#### 3.1.3 Introduction of Generalized Proof Generation/Verification and Its Rationale

In the original paper [1] and the related works [3, 6], the conventional Pietrzak halving protocol is repeated until the time parameter  $T$  gets 1 for proof generation. It helps the verifier consume the nearly least resources to verify VDF proofs in general systems. However, on Ethereum, the cost of resource usage, called gas, significantly differs from general environments. Ethereum Yellowpaper [8] provides predefined gas prices for transactions and opcodes executions. Especially in this context, repeating the halving protocol till  $T = 1$  does not guarantee the most efficient verification. Therefore, we generalized the Pietrzak verification algorithm with flexible repetition of the halving protocol. In Algorithm 4, we introduced a new parameter  $\delta$ . The halving protocol is repeated till the time variable becomes equal to  $\delta$ . Then, the verifier checks  $y \stackrel{?}{=} x^{2^{\delta}}$ .

### 3.1.4 Generalized Proof Generation

In Algorithm 3, the generalized proof generation is used to construct the cryptographic proofs required for VDF verification under flexible conditions. The proof generation starts with the evaluation result and halves the exponentiation of a proof step-by-step until reaching the specified parameter  $\delta$ . Each halving can be tracked as intermediate values  $v_i$  are stored as part of the proof. This mechanism allows for flexible adjustment of the verification process to accommodate different system capacities and security requirements.

---

#### Algorithm 3 Generalized Proof Generation of the Pietrzak VDF with Evaluation

---

```

1: input:  $x, T, \delta, N$ 
2: output:  $\{\pi_i\}_{i=1}^{\tau-\delta}$ 
3:  $\tau \leftarrow \lceil \log_2(T) \rceil$ 
4:  $y \leftarrow x$ 
5: for  $k \leftarrow 1$  to  $T$  do
6:    $y \leftarrow y^2 \bmod N$ 
7: end for
8:  $(x_1, y_1) \leftarrow (x, y)$ 
9: for  $i \leftarrow 1$  to  $\tau - \delta$  do
10:    $v_i \leftarrow x^{2^{T/2^i}}$ 
11:    $r_i \leftarrow \text{keccak256}(x_i + y_i + v_i)$ 
12:    $x_{i+1} \leftarrow x_i^{r_i} \cdot v_i \bmod N$ 
13:   if  $T/2^{i-1}$  is odd then
14:      $y_i \leftarrow y_i^2 \bmod N$ 
15:   end if
16:    $y_{i+1} \leftarrow v_i^{r_i} \cdot y_i \bmod N$ 
17:    $\pi_i \leftarrow v_i$ 
18: end for
19: return  $\{\pi_i\}_{i=1}^{\tau-\delta}$ 

```

---

### 3.1.5 Generalized Verification

Algorithm 4 describes the generalized verification process for VDFs on Ethereum. It utilizes the proofs generated by the generalized proof generation method to validate the sequence of operations leading to the final result. The verifier iteratively computes and checks each step of the proof against the corresponding intermediate values and the final condition  $y_{\tau-\delta+1} = x_{\tau-\delta+1}^{2^{\delta}}$ . This process ensures that the computation was performed correctly and meets the specified delay constraints, which is crucial for applications relying on the integrity of timed cryptographic operations.

According to Algorithm 3, and 4, the data should be submitted are the root ( $x$ ), the VDF evaluation result ( $y = x^{2^T}$ ), the time delay variable ( $T$ ), the VDF proof ( $\{\pi_i\}_{i=1}^{\tau-\delta}$ ), and the group description ( $N$ ) as described in Equation 2.

$$\left( N, x, y, \tau, \overbrace{(\pi_1, \pi_2, \pi_3, \dots, \pi_k)}^{\lceil \log_2(T) \rceil - \delta} \right) \quad (2)$$

## 3.2 Target Time Delay and the Bit Length

Recent advances in VDF implementation using C++, as studied by Attias et al. [3], demonstrate that VDF evaluation times can range from  $2^{20}$  to  $2^{25}$  cycles. These findings suggest that the implementations are not only effective but also efficient in experimental setups. In the context of Ethereum, where block generation typically requires around 12 seconds and even less time in other blockchain systems, we recommend that the time delay for generating VDF-based random numbers should not exceed one minute. This recommendation aims to prevent excessive resource consumption without compromising practical utility.

The experimental results from Attias et al. [3] show that a performance duration of approximately one minute at the 2048-bit level is feasible. Consequently, we advocate for a similar time range in VDF applications. The security of our target Pietrzak VDF configuration depends on the difficulty of the prime factoring problem, akin to that in the RSA

**Algorithm 4** Generalized Verification of the Pietrzak VDF

---

```

1: input:  $x, y, T, \delta, \{\pi_i\}_{i=1}^{\tau-\delta}, N$ 
2: output: True or False
3:  $\tau \leftarrow \lfloor \log_2(T) \rfloor$ 
4:  $(x_1, y_1) \leftarrow (x, y)$ 
5: for  $i \leftarrow 1$  to  $\tau - \delta$  do
6:    $v_i \leftarrow \pi_i$ 
7:    $r_i \leftarrow \text{keccak256}(x_i + y_i + v_i)$ 
8:    $x_{i+1} \leftarrow x_i^{r_i} \cdot v_i \bmod N$ 
9:   if  $T/2^{i-1}$  is odd then
10:     $y_i \leftarrow y_i^2 \bmod N$ 
11:   end if
12:    $y_{i+1} \leftarrow v_i^{r_i} \cdot y_i \bmod N$ 
13: end for
14: if  $y_{\tau-\delta+1} = x_{\tau-\delta+1}^{2^\delta}$  then
15:   return True
16: else
17:   return False
18: end if

```

---

encryption system. Currently, a 2048-bit key length is deemed sufficient for maintaining security standards. However, considering potential advancements in computational capabilities, a 3072-bit key length might be necessary after ten years. Therefore, our experiments included tests with both 2048-bit and 3072-bit settings for VDFs.

### 3.3 Environment for Gas Usage Measurement

Here we describe the setup of this research used to measure gas usage in Ethereum smart contracts, detailing the use of Solidity and the related framework.

#### 3.3.1 Development Environment and Compiler Version

The development of the contract was conducted using Solidity version 0.8.23. This choice was driven by the compatibility and full support provided by the Hardhat framework, a comprehensive Ethereum development environment with integrated debugging capabilities. At the start of the development process, Solidity 0.8.23 was the latest compiler version fully supported by Hardhat for debugging and other essential development functionalities. Generally, gas optimization is best achieved with the latest version of the compiler.

#### 3.3.2 Optimizer Configuration

For configuration, the core parameter of the Solidity optimizer is `Runs` which indicates how often each opcode will be used in the deployed contract. That is, higher `Runs` implies less gas cost for execution and higher gas cost for deployment. We set the optimizer parameter `Runs` to  $4,294,967,295(2^{32} - 1)$ , which is the maximum value of the parameter, indicating the highest level of optimization for execution.

We set up Via-IR (Intermediate Representation) and the Yul optimizer in the Solidity compiler to generate efficient bytecode. Via-IR helps efficiency, security, and simplicity in code generation by deviating from the direct compilation of Solidity code to EVM bytecode. Instead, via-IR processes an intermediate step where Yul code, an intermediate representation, is generated.

In this step, we can enhance the Yul optimizer's efficiency. We replaced the `msize()` operation with the free memory pointer. This adjustment necessitated manual updates to the memory indexes, a process rigorously tested to ensure the integrity of our implementation. We also applied memory-safe assembly blocks in our code. This change not only aligns with Solidity's memory model but also activates Via-IR in the compiler settings, resulting in significant gas savings.

#### 3.3.3 Gas Measurement

We implemented external functions in `MinimalApplication.sol`, the major source file for implementation, to measure the gas used with different strategies. The gas cost depends on the order of the function selectors in these

external functions, but the differences are considered to be negligible, with a maximum difference of about 60 gas used across the seven external functions. Therefore, an error margin of about 60 gas exists for the results presented in the figures.

### 3.3.4 Local Testing Environment

We utilized the Hardhat node, provided by the Hardhat framework, to create a local testing environment. The amount of gas usage was obtained using the `eth_estimateGas` method, which generates and returns an estimate of the gas required to complete the transaction. This method accurately measures the gas used in the execution of different contract functions and provides valuable insights into the efficiency of the implementations. It is important to note that the actual gas cost incurred on the real network is determined by multiplying the estimated `gasUsed` by the `gasPrice` at the Ethereum network circumstance.

## 4 Data and Accompanying Gas Cost

In this section, we introduce the data structure we used to send VDF proofs in the Ethereum transaction calldata. Then, we investigate the gas cost to send VDF proofs and regress the results to linear functions for the next sections.

### 4.1 Data Structure

In this study, the VDFs are implemented with key sizes of 2048 and 3072 bits. However, the EVM natively supports arithmetic operators only up to 256-bit numbers. Therefore, to facilitate efficient computation of numbers exceeding 256 bits, it is necessary to employ customized data formats. We revised the big number library implementation for Solidity developed by Firo [9]. The original data structure in this library includes bytes data (bytes `val`), bit length (`uint bitlen`), and a sign indicator (`bool neg`). Among the three elements, we deleted the sign indicator and its related low-level logic since our implementation does not require handling negative values. This library optimizes on-chain operations such as addition and subtraction by adding leading zeros for 32-byte alignment with the EVM's memory word size, eliminating offset management. Also, it utilizes the bit length data field to optimize multiplication and comparison operations. Therefore, we format the bytes data and pre-calculate bit length off-chain before submission, significantly reducing unnecessary on-chain computations. For example, the data format for a 2048-bit representation in JSON is as shown in Listing 1. In this way, we can reduce the gas cost even though the calldata size increases. This decision is reasonable because the primary goal is to reduce the gas cost, not the transaction calldata size.

**Listing 1** Calldata for a Big Number Example

```

1  {
2      "big_number": {
3          "val": "0x4621c26320fe0924bba1b7d5bc863495b9f0db3823b12a9a18e21
4              d23.....b2127fd6390f5f6234a164bd39d1dd6884b768c4dd790586ee",
5          "bitlen": 2047
6      }

```

### 4.2 Gas Cost of Calldata

The gas cost for Ethereum transaction calldata was fixed in EIP-2028 "Transaction data gas cost reduction" [10]. According to the document, the cost of calldata is divided into two cases:

- Non-zero byte: 16 gas
- Zero byte: 4 gas

Considering the above gas pricing, we can calculate the cost for sending one 2048-bit length data in the aforementioned data structure. 2048-bit data is transformed into 512-length hex letters.

In our implementation, the function `verifyRecursiveHalvingProof` processes the generalized verification (Algorithm 4). It is defined as the Listing 2 in Solidity codes.

**Listing 2** Interface of the Halving Verification Function

---

```

1 function verifyRecursiveHalvingProof(
2     BigNumber[] memory v,
3     BigNumber memory x,
4     BigNumber memory y,
5     BigNumber memory n,
6     uint256 delta,
7     uint256 T
8 )

```

---

A call to this function involves encoding parameter values. Start by computing the keccak256 of the UTF-8 byte representation of the string<sup>1</sup> based on Listing 2 and use the first four bytes, which results in 0xd8e6ac60.

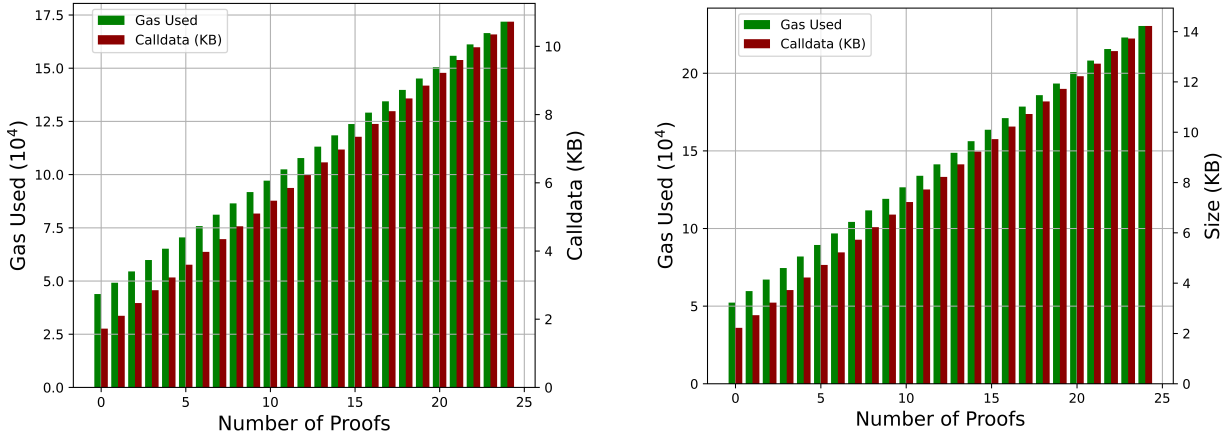
For static types such as `uint256`, fields including `delta` and `T` are padded to 32 bytes. For dynamic types including `bytes`, `struct`, and dynamic arrays, they are encoded by specifying an offset to the start of its data area, followed by the length of the data and the actual data. In case of `BigNumber[] memory v`, it is the dynamic array of dynamic type `struct BigNumber` that contains dynamic bytes `val`. So the way dynamic types are encoded is recursively applied to each halving proof `v`.

In EVM, dynamic types such as arrays and structs are encoded by specifying an offset to the start of the data, its length, and then the data itself. This method applies recursively for nested dynamic types. Parameters such as  $T$ ,  $\delta$ ,  $\lambda$ , and parameter count (e.g., 6 in our model) determine the offsets and lengths. The gas usage for data depends probabilistically on the distribution of zero and non-zero bytes in the data. Since EVM organizes memory in 32-byte words, we can consider the same number of word is repeated when data is repeated. Finally, we can predict the approximate gas usage of calldata using this EVM data construction structure.

Considering the precision of data and its cost, we performed experiments to test the size of calldata and the related gas usage. The related gas usage comprises of the intrinsic gas and data dispatching gas. The intrinsic gas in EVM refers the minimum cost for a transaction. It contains the transaction cost and the cost for data allocation. For verification, we need not only to allocate data in a transaction, but also to dispatch data into the verification function. The dispatching cost is proportional to the data size. Therefore, we decided to include the dispatching cost into the data cost in this study. Figure 2a for  $\lambda = 2048$  and 2b for  $\lambda = 3072$  show the calldata size with the number of proofs and the related gas usage. We can see the gas usage and the calldata size simply and linearly increase with the number of proofs.

<sup>1</sup>verifyRecursiveHalvingProof((bytes,uint256)[],(bytes,uint256),(bytes,uint256),(bytes,uint256),uint256,uint256)

Figure 2: Experiment results of the calldata length and cost for the proofs

(a) Calldata size and gas cost including intrinsic gas and dispatching gas ( $\lambda = 2048$ )(b) Calldata size and gas cost including intrinsic gas and dispatching gas ( $\lambda = 3072$ )

Finally, to elucidate the relationship between transaction size and gas costs, we perform a regression analysis. By applying the least squares method to approximate the best fit, we derive the following linear regression equations 3 and 4 for data sizes of 2048 and 3072 bytes, respectively:

$$G_{data,2048}(\tau) = 5295.73 \cdot \tau + 37610.11 \quad (3)$$

$$G_{data,3072}(\tau) = 7389.31 \cdot \tau + 43943.88 \quad (4)$$

These equations estimate the gas cost  $G$  as a function of transaction size  $\tau$ , highlighting the increase in required gas with larger transaction calldata.

## 5 Arithmetic Operations and Accompanying Gas Cost

This section focuses on analyzing the expenses associated with performing arithmetic operations in the context of verifying the Pietrzak VDF. The cost consists of two components: the cost of repeated halving and the cost of modular exponentiation for the final check. The algorithm executes a halving operation and then proceeds with a modular exponentiation verification. The modular exponentiation cost is studied before the halving cost, as the halving process includes the modular exponentiation. Using the results, we perform a regression analysis to formulate mathematical equations for the cost in the section that follows.

### 5.1 Modular Exponentiation Cost

This part explores strategies for optimizing the computational cost of modular exponentiation, a frequent operation in various cryptographic algorithms. It discusses algorithms such as Square and Multiply [11], Dimitrov multiexponentiation [12], and the ModExp contract introduced by EIP-198.

#### 5.1.1 Square and Multiply

The square and multiply algorithm, also called binary exponentiation, is an efficient approach for computing exponentiation operations  $x^n$ , particularly beneficial for large number modular exponentiation. As described in Algorithm 5, by converting the exponent  $b$  into its binary representation, the algorithm optimizes computation through a series of square (squaring) and multiply (multiplying by the base  $x$ ) operations based on the binary digits of  $n$ . For an exponent represented by  $k$  bits, the algorithm requires at most  $k - 1$  squaring and  $k - 1$  multiplication operations, making the computational complexity  $O(\log_2 n)$ . This optimization is simple but significantly enhances efficiency for large-scale modular exponentiation tasks.

---

#### Algorithm 5 Square and Multiply for Modular Exponentiation

---

```

1: input:  $a, b, N$ 
2: output:  $a^b \bmod N$ 
3:  $r \leftarrow 1$ 
4:  $a \leftarrow a \bmod N$ 
5: while  $b > 0$  do
6:   if  $b \bmod 2 = 1$  then
7:      $r \leftarrow (r \cdot a) \bmod N$ 
8:   end if
9:    $b \leftarrow b \gg 1$ 
10:   $a \leftarrow (a \cdot a) \bmod N$ 
11: end while
12: return  $r$ 

```

---

#### 5.1.2 Dimitrov Multiexponentiation

The Dimitrov algorithm [3, 12] presented in Algorithm 6 enhances the efficiency of large integer multiplication, crucial in fields such as cryptography and computational mathematics, by significantly reducing the computational complexity. Traditionally, the multiplication of large integers ( $x^a y^b$ ) exhibits a complexity of  $O(2 \log_2 \max(a, b))$ . Utilizing the binary exponentiation method [13], the Dimitrov algorithm achieves a computational complexity closer

to  $O(\frac{7}{4} \log_2 \max(a, b))$ . This characteristic allows for the rapid and resource-efficient multiplication of very large integers, making the algorithm particularly valuable for applications requiring efficient large-scale numerical operations. In the generalized verification (Algorithm 4), lines 9 – 12 perform multiexponentiation only if  $T/2$  is odd. Therefore, we considered the Dimitrov algorithm as a candidate algorithm to apply for optimization.

---

**Algorithm 6** Dimitrov Multiexponentiation Algorithm
 

---

```

1: input:  $x, y, a, b, N$ 
2: output:  $x^a \cdot y^b \pmod{N}$ 
3:  $h \leftarrow \max(\lfloor \log_2 a \rfloor + 1, \lfloor \log_2 b \rfloor + 1)$ 
4:  $z \leftarrow 1$ 
5:  $q \leftarrow x \cdot y \pmod{N}$ 
6: for  $i = h - 1$  down to 0 do
7:    $z \leftarrow z \cdot z \pmod{N}$ 
8:   if  $a_i = 1$  and  $b_i = 0$  then
9:      $z \leftarrow z \cdot x \pmod{N}$ 
10:   else if  $a_i = 0$  and  $b_i = 1$  then
11:      $z \leftarrow z \cdot y \pmod{N}$ 
12:   else if  $a_i = 1$  and  $b_i = 1$  then
13:      $z \leftarrow z \cdot q \pmod{N}$ 
14:   end if
15: end for
16: return  $z$ 
  
```

---

### 5.1.3 ModExp by EIP-198

EIP-198 [14], known for introducing "Big Integer Modular Exponentiation", introduces the ModExp (Modular Exponential) precompiled contract to the EVM, offering a streamlined and cost-efficient approach to conducting large integer modular exponentiation, a foundational operation in numerous cryptographic algorithms.

This function calculates  $a^b \pmod{n}$ , where  $a$ ,  $b$ , and  $n$  are large numbers, and prior to EIP-198, such execution on-chain was not officially supported by any operations. The ModExp contract mitigates these expenses by providing a standardized computation method, thus facilitating the incorporation of cryptographic computations within smart contracts. Building on this, EIP-2565 [15] contributed to further refining the gas cost model for these modular exponentiation operations by proposing adjustments to the pricing formula.

### 5.1.4 Comparison of Exponentiation Techniques and Regression

Figure 3a and Figure 3b present the gas usage experiment results of three modular exponentiation techniques. We name a naive exponentiation approach as exponentiation by squaring in the figures. Even if square and multiply (Algorithm 5) reduces the gas usage, it is obvious that the precompiled ModExp uses outstandingly less gas for the modular exponentiation than the others. Figure 3c and Figure 3d show the gas usage experiment results for modular multiexponentiation. We implemented Dimitrov multiexponentitaion including the precompiled ModExp. The comparing data named 'Precompile' is the gas usage when only the precompiled ModExp is used for multiexponentiation. The latter takes significantly less gas than the Dimitrov algorithm. Therefore, we applied ModExp for both the modular exponentiation and multiexponentiation operations in the implementation in Algorithm 4.

In the experiment, the pricing of ModExp is linearly proportional to the number of exponentiation as  $\mathcal{G}(T) = aT + b$ . As Equation 1, we denote  $\tau$  as the logarithmic value of  $T$ . We could get the following results from a simple regression process.

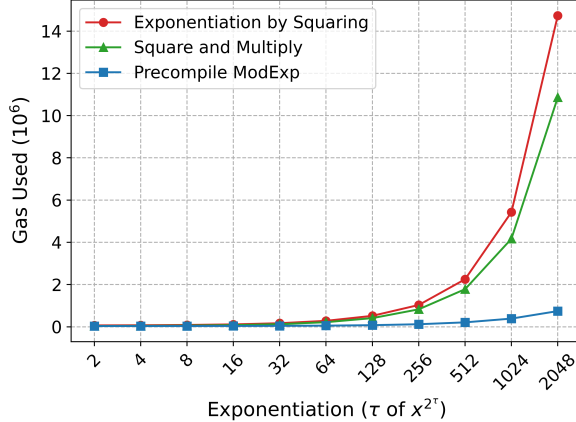
$$\mathcal{G}_{exp,2048}(\tau) = 346.92 \cdot 2^\tau + 33432.08 \quad (5)$$

$$\mathcal{G}_{exp,3072}(\tau) = 780.83 \cdot 2^\tau + 37445.60 \quad (6)$$

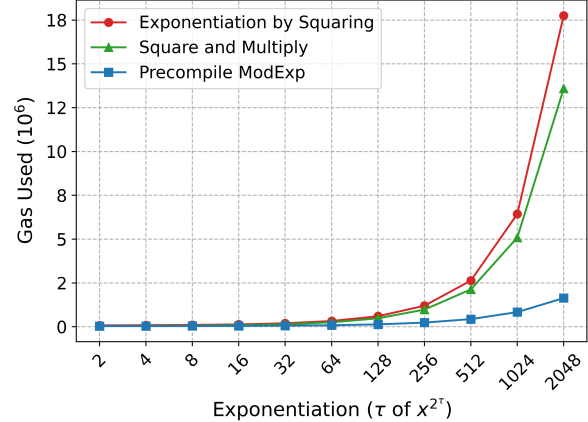
## 5.2 Halving Cost

The halving cost of the arithmetic operations in the verification indicates the gas usage for lines 5 – 13 in Algorithm 4. The modular exponentiation operations in lines 8, 10, and 12 use the precompiled ModExp since its best efficiency in

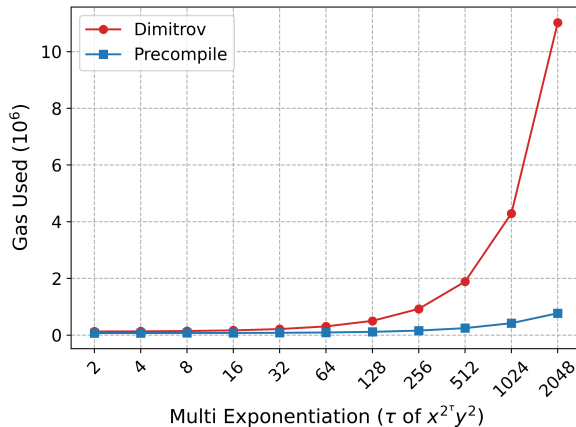
Figure 3: Experiment results of the modular exponentiation cost



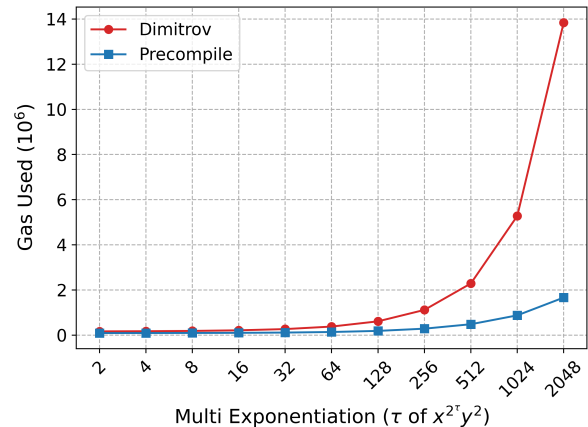
(a) Gas usage of exponentiation by squaring, square and multiply, and precompiled ModExp, x is 2048-bit level



(b) Gas usage of exponentiation by squaring, square and multiply, and precompiled ModExp, x is 3072-bit level



(c) Gas usage of Dimitrov multiexponentiation and only precompiled ModExp, x is 2048-bit level



(d) Gas usage of Dimitrov multiexponentiation and only precompiled ModExp, x is 3072-bit level

the previous subsection. For simplicity, as we assumed  $T = 2^\tau$ , in this case, the if statement in line 9 is always false, therefore line 10 is never executed. Hence, the gas usage will be clearly proportional to the number of the repetition time, that is,  $\tau - \delta$ .

The results of our experiments demonstrate the anticipated correlation. Figure 4a and Figure 4b display the gas cost of the repeated halving operations with  $\lambda = 2048$  and  $\lambda = 3072$  correspondingly. The data exhibits a clear linear relationship, allowing us to perform a regression analysis and model the results using a linear function. By employing the method of least squares approximation, we obtain the subsequent functions as Equation 7 and 8:

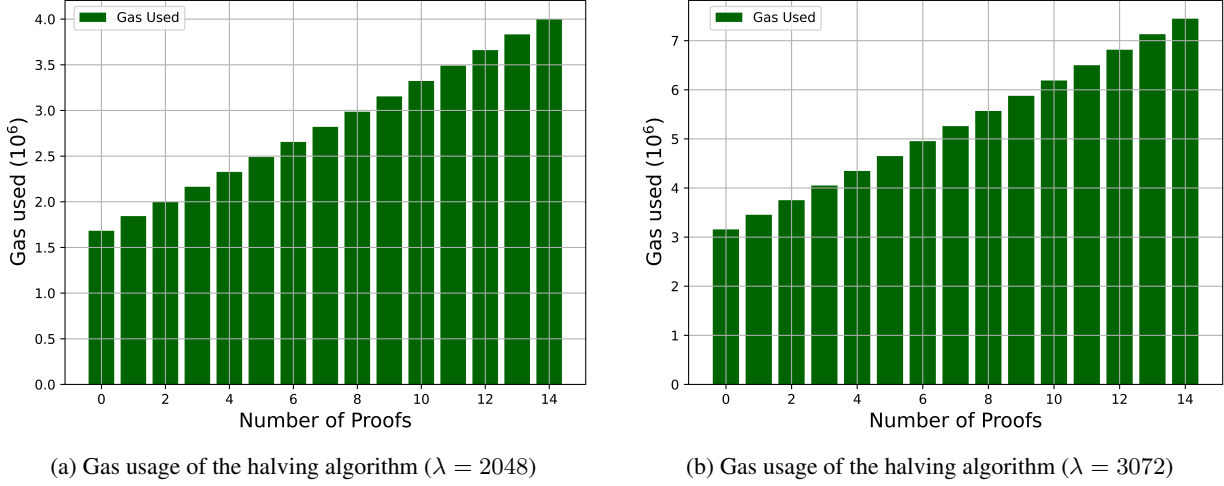
$$G_{\text{halving},2048}(\tau) = 165482.26 \cdot \tau - 155642.3 \quad (7)$$

$$G_{\text{halving},3072}(\tau) = 306089.32 \cdot \tau - 238572.65 \quad (8)$$

## 6 Cost-Effective Implementation

This section explains the implementation of a cost-efficient Pietrzak VDF verifier as an Ethereum smart contract. In the beginning, we utilize the gas cost outcomes obtained from the preceding sections to make theoretical predictions for the optimized proof generating process. Secondly, we prove that there exists a unique  $\delta$  that minimizes the gas usage for

Figure 4: Experiment results of the halving repetition cost



VDF verification, and this minimization is independent of  $\tau$ . In the end, we compare the anticipated outcome based on theory with the actual results obtained from the experiment.

### 6.1 Theoretical Analysis on Proof Generation for Gas Usage Optimization

The optimized proof generation in this research means minimizing the verification gas cost. We can define the total gas cost function  $\mathcal{G}_{total}$  using the previous regression results.

$$\mathcal{G}_{total}(\tau, \delta) = \mathcal{G}_{calldata} + \mathcal{G}_{halving} + \mathcal{G}_{exp} + C \quad (9)$$

$$= (\alpha \cdot (\tau - \delta) + c_1) + (\beta \cdot (\tau - \delta) + c_2) + (\gamma \cdot 2^\delta + c_3) + C \quad (10)$$

$$= (\alpha + \beta)(\tau - \delta) + \gamma \cdot 2^\delta + C' \quad (11)$$

Then, we get Theorem 1 says that there is a unique delta minimizing the total gas cost.

**Theorem 1.** *The function  $\mathcal{G}_{total}(\tau, \delta)$  has exactly one unique minimum for  $\delta$  when  $\tau > \delta = \log_2(\alpha + \beta) - \log_2(\ln 2 \cdot \gamma)$ .*

*Proof.* Firstly, we calculate the partial derivative of  $\mathcal{G}_{total}$  with respect to  $\delta$ , which yields

$$\frac{\partial \mathcal{G}_{total}}{\partial \delta} = \ln 2 \cdot \gamma \cdot 2^\delta - (\alpha + \beta).$$

To show that there is a unique  $\delta$  that minimizes  $\mathcal{G}_{total}$ , we need to find where this derivative equals zero. This leads us to the equation

$$2^\delta = \frac{\alpha + \beta}{\ln 2 \cdot \gamma}.$$

The function  $2^\delta$  is strictly increasing. Hence, the equation  $2^\delta = \frac{\alpha + \beta}{\ln 2 \cdot \gamma}$  has a unique solution  $\delta$ , which can be expressed as

$$\delta = \log_2(\alpha + \beta) - \log_2(\ln 2 \cdot \gamma).$$

This  $\delta$  is where the first derivative equals zero.

Further, to confirm that this  $\delta$  is indeed a minimum, we need to check the second derivative. The monotonic nature of the exponential function in this context implies that as  $\delta$  increases,  $\gamma \cdot 2^\delta$  grows without bounds, while decreasing  $\delta$  below this point leads to  $\gamma \cdot 2^\delta$  becoming smaller than  $\alpha + \beta$ , thereby confirming that the function is minimized at this  $\delta$ .

Thus,  $\mathcal{G}_{total}(\tau, \delta)$  indeed has one unique minimum at  $\delta$  within the specified range of  $\tau > \delta \geq 0$ , completing the proof.  $\square$

Also, we denote the minimizing  $\delta$  as

$$\delta_m = \arg \min_{\delta} \mathcal{G}_{total}(\tau, \delta). \quad (12)$$

From Theorem 1, we can get the unique  $\delta_m$  optimizing the gas cost. Applying all the regression results in Equation 3, 4, 5, 6, 7, and 8, we get the optimizing  $\delta_m \approx 9.47$  for  $\lambda = 2048$  and  $\delta_m \approx 9.18$  for  $\lambda = 3072$  respectively. In practice,  $\delta$  for implementation must be an integer. Therefore, we can get the practical integer  $\delta$  with the following corollary.

**Corollary 2.** *Let  $\delta_m$  be a real number, and let  $\mathcal{G}(\tau, \delta)$  denote a function in  $\tau$  and  $\delta$ . Define  $\Delta = \delta_m - \lfloor \delta_m \rfloor$  as the fractional part of  $\delta_m$ . Then, the relationship between  $\mathcal{G}(\tau, \lfloor \delta_m \rfloor)$  and  $\mathcal{G}(\tau, \lceil \delta_m \rceil)$  depends on  $\Delta$  as follows:*

1. *If  $\Delta < -\log_2(\ln 2)$ , then  $\mathcal{G}(\tau, \lfloor \delta_m \rfloor) < \mathcal{G}(\tau, \lceil \delta_m \rceil)$ .*
2. *If  $\Delta = -\log_2(\ln 2)$ , then  $\mathcal{G}(\tau, \lfloor \delta_m \rfloor) = \mathcal{G}(\tau, \lceil \delta_m \rceil)$ .*
3. *If  $\Delta > -\log_2(\ln 2)$ , then  $\mathcal{G}(\tau, \lfloor \delta_m \rfloor) > \mathcal{G}(\tau, \lceil \delta_m \rceil)$ .*

*Proof.* Define

$$f(\delta) = \mathcal{G}(\tau, \delta + 1) - \mathcal{G}(\tau, \delta) = \gamma \cdot (2^{\delta+1} - 2^\delta) + (\alpha + \beta)(-(\delta + 1) + \delta) = \gamma \cdot 2^\delta - (\alpha + \beta). \quad (13)$$

Then,  $f(\delta) = 0$  when

$$\delta = \log_2(\alpha + \beta) - \log_2 \gamma. \quad (14)$$

Also, as given  $\gamma > 0, \delta > 0$

$$\frac{df}{d\delta} = \ln 2 \cdot \gamma \cdot 2^\delta, \quad (15)$$

$f$  is a monotone-increasing function in the boundary. Therefore, after the point  $\delta'$  where

$$\delta' = \log_2(\alpha + \beta) - \log_2 \gamma = \delta_m + \log_2(\ln 2), \quad (16)$$

$f$  is bigger than 0.

For the 1st case of the lemma,  $\Delta < -\log_2(\ln 2)$  implies

$$f(\lfloor \delta_m \rfloor) > 0. \quad (17)$$

As the definition of  $f$ ,

$$\mathcal{G}(\tau, \lfloor \delta_m \rfloor) < \mathcal{G}(\tau, \lceil \delta_m \rceil). \quad (18)$$

In the same way, we can get the other two cases.  $\square$

Since  $\log_2(\ln 2) \approx -0.52$ , the optimal integer value of  $\delta$  is 9 for both  $\lambda = 2048$  and  $3072$ , as the 1st case of Corollary 2.

## 6.2 Optimized Verification Gas Cost

Figures 5a and 5b depict the total gas cost for Pietrzak VDF verification at  $\lambda = 2048$  and  $\lambda = 3072$  respectively. Consistent with the theoretical predictions in Theorem 1, the gas usage graph shows a decline to a minimal point before increasing sharply. Optimal gas costs were observed at  $\delta = 9$  for both configurations, aligning perfectly with the findings of Corollary 2. This alignment between theoretical expectations and empirical results confirms the accuracy of our model and highlights its potential for optimizing Pietrzak VDF verification in blockchain applications.

Table 1 details the gas consumption and `calldata` sizes for the implemented parameters, uniformly using  $\delta = 9$ . Contrary to the previous expectation of `calldata` sizes around 40KB [3], the sizes recorded were significantly lower, ranging from 5.52 to 7.35 KB for  $\lambda = 2048$  and from 7.22 to 9.72 KB for  $\lambda = 3072$ . Gas usage varied from 1.96 to 2.80 million for  $\lambda = 2048$  and from 3.68 to 5.26 million for  $\lambda = 3072$ . These findings not only demonstrate the efficacy of our approach but also highlight potential areas for further optimization in VDF implementations. Such improvements could lead to significant cost reductions in blockchain networks, enhancing the overall efficiency of cryptographic operations.

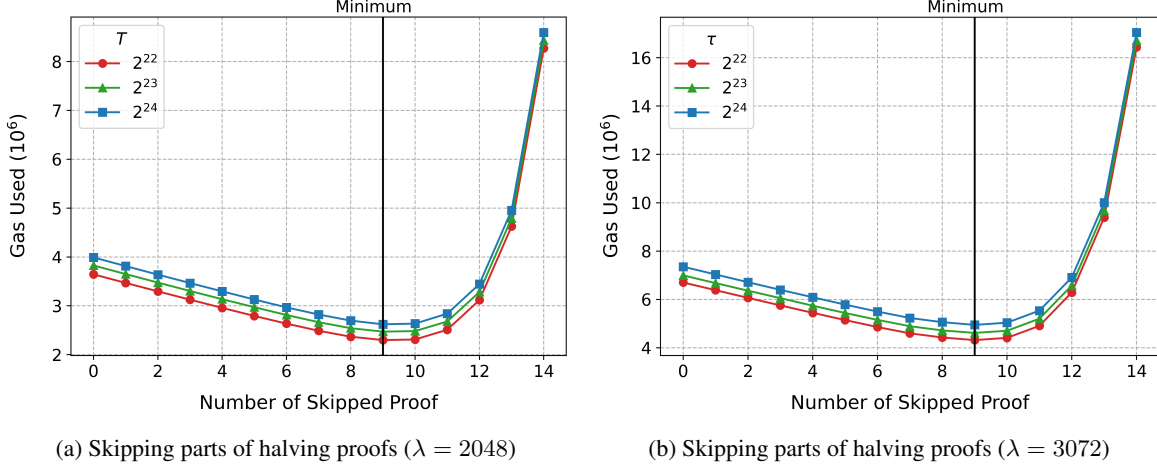
Figure 5: Experiment results for halving proof skipping parameter  $\delta$  with  $\tau = 22, 23, 24$ 

Table 1: Implementation results based on the analysis

$\lambda$	$\delta$	$\tau$	Gas used	Calldata size (KB)
2048	9	20	1970844	5.38
		21	2133372	5.75
		22	2297629	6.13
		23	2470594	6.50
		24	2620907	6.89
		25	2799805	7.25
3072	9	20	3680363	7.13
		21	3967114	7.63
		22	4318050	8.13
		23	4614955	8.63
		24	4947040	9.13
		25	5254521	9.63

## 7 Discussion

This section discusses the implementation of VDFs on Ethereum, focusing on programming choices for Ethereum’s Virtual Machine and their impact on gas optimization. We introduce challenges associated with VDF deployment on Ethereum’s Layer 1 due to high costs and explore Layer 2 solutions. The discussion concludes with an analysis of economic factors critical for VDF integration and sustainability on the blockchain.

### 7.1 Implementation Languages

There are main development languages in EVM-compatible network environments, for example, Viper, Huff, Solidity, and Yul. For our implementation, which requires dynamically adjusting proof lengths, we excluded Vyper due to its inability to handle dynamic data structures efficiently. Instead, we chose Solidity combined with Yul, leveraging Solidity for its comprehensive features and developer familiarity, and Yul for its superior gas optimization capabilities. This combination provides a balance between high-level language safety and low-level control over the Ethereum Virtual Machine.

Considering future enhancements, we are exploring Huff, noted for its exceptional gas efficiency and direct control over the EVM. Huff originated from the Aztec team where contracts needed extreme efficiency, even more than what Yul could provide. Although Huff offers significant optimization opportunities, it lacks the built-in safety checks of higher-level languages, raising the implementation complexity. Nevertheless, given our implementation’s emphasis on gas optimization, the benefits of adopting Huff justify its consideration for future development.

## 7.2 Practicality of VDF on EVM

Implementing VDFs on Ethereum’s Layer 1 presents significant challenges primarily due to high gas costs and the computational intensity required. Our detailed optimization trials reveal that despite employing cutting-edge optimization techniques, verifying a Pietrzak VDF on Layer 1 still demands at least one million gas units. This high resource consumption makes VDF applications impractical for widespread use on Ethereum’s primary network, especially for operations requiring frequent and repetitive VDF verifications. The economic implications of these requirements can stifle innovation and discourage developers from incorporating VDFs into their decentralized applications, limiting the exploration of potentially valuable use cases such as randomized governance protocols or secure public randomness in blockchain networks.

However, the emergence of Layer 2 solutions, such as optimistic rollups and zkRollups, offers a promising alternative for leveraging VDFs within the Ethereum ecosystem. These technologies provide a secondary processing layer that can handle complex computations off the main Ethereum chain, thereby significantly reducing gas costs and improving transaction throughput. Platforms like Optimism capitalize on these advantages, offering gas prices that are often thousands of times cheaper than those on Layer 1. This dramatic cost reduction opens up new possibilities for using VDFs on Ethereum, allowing for more frequent and economically viable implementations. Layer 2 solutions not only mitigate the high cost barriers associated with Layer 1 but also broaden the scope for adopting VDFs in a variety of applications, thus encouraging further development and research into this promising area of blockchain technology.

## 7.3 Lack of Economic VDF Protocols in Ethereum

The integration of VDFs into smart contracts holds great promise for enhancing blockchain security and reliability. However, beyond the technical challenges, there exists a substantial hurdle in the lack of a robust economic model specifically designed to support the unique operational needs of VDFs, such as incentivizing both provers and verifiers and managing commit-reveal-recover protocols. The absence of such an economic framework complicates the practical deployment of VDFs as it does not adequately address compensation for participants who dedicate substantial computational resources to generate and verify proofs. This gap can deter the participation of potential contributors, ultimately hindering the scalability and effectiveness of VDFs in real-world blockchain applications.

Moreover, considering the decentralized essence of blockchain technology, it is crucial that any protocol, especially those as intricate as VDFs, is underpinned by an economic strategy that not only supports technical execution but also ensures economic sustainability without the need for central governance. This calls for innovative research into economic models that are specifically tailored to the decentralized context of blockchain networks. These models need to effectively balance incentives and deterrence, fostering a system where honest participation is rewarded while dishonest behavior is penalized. Such economic strategies are vital for maintaining the integrity and fairness of the blockchain ecosystem, ensuring that VDFs are not only technically feasible but also economically viable and beneficial to all participants, thereby aligning with the overarching principles of decentralization and trust minimization in blockchain systems.

## 7.4 Future Works on a General Environment

Through this research, we investigated the efficient implementation of Pietrzak VDF verification within the Ethereum Virtual Machine (EVM) environment and observed results that align both theoretically and experimentally. During our study, we identified significant effects of generalized proof generation and verification, which were also included within the predictable realms of theoretical analysis. We anticipate that such an approach could be applicable not only within the EVM but also in more general computing environments. Although resource pricing in general systems would differ from the gas costs in the EVM, with elements like the repetition of halving protocols and resource consumption proportional to the proof length being predictable, the costs of exponentiation in VDF ( $2^{2^T}$ ) are expected to be exponential. Therefore, based on the outcomes of this study, further research on optimizing Pietrzak VDFs in general computing environments appears reasonable.

## 8 Conclusion

In conclusion, our research has successfully demonstrated the feasibility and significance of implementing VDFs within blockchain environments, particularly through smart contracts in Ethereum. By focusing on the Pietrzak VDF construction, we have not only bridged a crucial gap in the academic studies of VDFs but also highlighted their practical utility in enhancing the security and efficiency of blockchain applications. Contrary to previous expectations, our work represents the first academic result in the cost-effective on-chain verification of the Pietrzak VDF, showing significant potential in ensuring cryptographically secure random number generation across various blockchain applications. Through strategic implementation, we have achieved substantial cost reductions, making the Pietrzak VDF more accessible and applicable. This research opens new avenues for the integration of VDFs in blockchain systems, promising to enhance security, fairness, and functionality in the evolving distributed ledger technologies.

## References

- [1] K. Pietrzak, “Simple verifiable delay functions,” in *10th innovations in theoretical computer science conference (itcs 2019)*, Schloss-Dagstuhl-Leibniz Zentrum für Informatik, 2019.
- [2] B. Wesolowski, “Efficient verifiable delay functions,” in *Advances in Cryptology–EUROCRYPT 2019: 38th Annual International Conference on the Theory and Applications of Cryptographic Techniques, Darmstadt, Germany, May 19–23, 2019, Proceedings, Part III* 38, pp. 379–407, Springer, 2019.
- [3] V. Attias, L. Vigneri, and V. Dimitrov, “Implementation study of two verifiable delay functions,” *Cryptology ePrint Archive*, 2020.
- [4] D. Boneh, J. Bonneau, B. Bünz, and B. Fisch, “Verifiable delay functions,” in *Annual international cryptology conference*, pp. 757–788, Springer, 2018.
- [5] R. L. Rivest, A. Shamir, and D. A. Wagner, “Time-lock puzzles and timed-release crypto,” 1996.
- [6] D. Boneh, B. Bünz, and B. Fisch, “A survey of two verifiable delay functions,” *Cryptology ePrint Archive*, 2018.
- [7] K. Choi, A. Arun, N. Tyagi, and J. Bonneau, “Bicorn: An optimistically efficient distributed randomness beacon,” in *Financial Cryptography and Data Security: 27th International Conference, FC 2023, Bol, Brač, Croatia, May 1–5, 2023, Revised Selected Papers, Part I*, (Berlin, Heidelberg), p. 235–251, Springer-Verlag, 2023.
- [8] G. Wood, “Ethereum: A secure decentralised generalised transaction ledger eip-150 revision (705168a - 2024-03-04),” 2017. Accessed: 2024-05-10.
- [9] firo, “Full bignumber library implementation for solidity.” <https://github.com/firoorg/solidity-BigNumber>, 2024. Accessed: 2024-05-10.
- [10] A. Akhunov, E. Ben Sasson, T. Brand, L. Guthmann, and A. Levy, “Eip-2028: Transaction data gas cost reduction.” Ethereum Improvement Proposals, 2019. Accessed: 2024-05-10.
- [11] A. J. Menezes, P. C. Van Oorschot, and S. A. Vanstone, *Handbook of applied cryptography*. CRC press, 2018.
- [12] V. S. Dimitrov, G. A. Jullien, and W. C. Miller, “Complexity and fast algorithms for multiexponentiations,” *IEEE Transactions on Computers*, vol. 49, no. 2, pp. 141–147, 2000.
- [13] C. K. Koc, “High-speed rsa implementation,” tech. rep., Technical Report TR-201, RSA Laboratories, 1994.
- [14] V. Buterin, “Eip-198: Big integer modular exponentiation.” Ethereum Improvement Proposals, 2017. Accessed: 2024-05-10.
- [15] K. Olson, S. Gulley, S. Peffers, J. Drake, and D. Feist, “Eip-2565: Modexp gas cost.” Ethereum Improvement Proposals, 2020. Accessed: 2024-05-10.